more complicated, because not only standard representations but projective representations also occur.

Finally, a basis for the full state space can be constructed as follows. The group of $\boldsymbol{k}$ is a subgroup of the space group G. G can be decomposed according to

$$G = G_{\boldsymbol{k}} + g_2 G_{\boldsymbol{k}} + \cdots + g_s G_{\boldsymbol{k}}$$

where the space group elements g_i have homogeneous parts R_i for which $R_i\boldsymbol{k} = \boldsymbol{k}_i$. Then the basis is defined as

$$\Psi_{ij} = T_{gi}\psi_j \qquad [23]$$

The dimension of the representation is sd, where s is the number of points $\boldsymbol{k}_i$, and d the dimension of the point group representation $D(K_{\boldsymbol{k}})$. The irreducible representation carried by the state space then is characterised by the so-called "star" of $\boldsymbol{k}$ (all vectors $\boldsymbol{k}_i$), and an irreducible representation of the point group $K_{\boldsymbol{k}}$. This means that electronic states and phonons can be characterized by $\boldsymbol{k}$, v. Their transformation properties under space group transformations follows from this characterization.

Aperiodic Crystals

Apart from crystals with three-dimensional lattice periodicity, there are materials with a diffraction pattern with sharp Bragg peaks on positions

$$\boldsymbol{k} = \sum_{i=1}^{n} h_i \boldsymbol{a}_i^* \quad (\text{integer } h_i) \qquad [24]$$

When $n = 3$, the structure is periodic. If $n > 3$, the structure is aperiodic, but it is still considered as crystal, because there is long-range order. Examples are modulated phases and quasicrystals. They may be described as intersections of physical space with a higher-dimensional lattice periodic structure. The symmetry of such structures is a space group in n dimensions, and in this case the theory of space groups in arbitrary dimensions can be used.

See also: Crystal Structure; Electron–Phonon Interactions and the Response of Polarons; Group Theory; Insulators, Electronic States of; Lattice Dynamics: Vibrational Modes; Periodicity and Lattices; Point Groups; Quantum Mechanics: Foundations; Quasicrystals; Scattering, Elastic (General).

PACS: 61.50.Ah; 02.30. – a

Further Reading

Cornwell JF (1997) *Group Theory in Physics*. San Diego: Academic Press.

Hahn Th. (ed.) (1992) *Space-Group Symmetry*. In: International Tables for Crystallography. vol. A, Dordrecht: Kluwer.

Hahn T and Wondratschek H (1994) *Symmetry of Crystals: Introduction to International Tables for Crystallography. vol. A*. Sofia, Bulgaria: Heron Press.

Janssen T (1973) *Crystallographic Groups*. North-Holland: Amsterdam.

Janssen T, Janner A, Looijenga-Vos A, and de Wolff PM (1999) *Incommensurate and commensurate modulated structures*. In: Wilson AJC and Prince E, *International Tables for Crystallography, vol. C, Mathematical, physical and chemical tables*. ch. 9.8, Dordrecht: Kluwer.

Nomenclature

$\boldsymbol{a}$, $\boldsymbol{b}$, $\boldsymbol{c}$	lattice basis vectors
$\boldsymbol{a}^*$, $\boldsymbol{b}^*$, $\boldsymbol{c}^*$	reciprocal lattice basis vectors
A	translation subgroup of a space group
$D(R)$	matrix representation
$\exp(-i\boldsymbol{k}\cdot\boldsymbol{r})U(\boldsymbol{r})$	Bloch form of a wave function
$E(3)$	Euclidean group
$F(\boldsymbol{k})$	structure factor
G	space group
K	point group
$\boldsymbol{n}$	lattice translation vector
$O(3)$	orthogonal group in three dimensions
$\boldsymbol{r}_j$	position of an atom in the unit cell
R	orthogonal transformation
$\{R\|\boldsymbol{t}\}$	space group element
T_g	linear operator for group element g:
$\hat{\rho}(\boldsymbol{k})$	Fourier component of $\rho(\boldsymbol{r})$
$\rho(\boldsymbol{r})$	density function
ψ_i	basis of a state space
$\psi(\boldsymbol{r})$	wave function

Specific Heat

N E Phillips and R A Fisher, University of California at Berkeley, Berkeley, CA, USA

Introduction

The specific heat of a substance is the amount of heat required to raise the temperature by one degree. When heat is introduced under certain specified conditions, it is a well-defined thermodynamic property that gives a measure of the increases in the entropy, the energy, and the enthalpy with increasing temperature. It is related to other thermodynamic properties, for example, the thermal expansion, which is a measure of the pressure dependence of the entropy. Specific-heat data make an important contribution to

the determination of the Gibbs and Helmholtz energies, the thermodynamic properties that govern the direction of spontaneous change and the equilibrium conditions for chemical reactions and phase transitions. When interpreted in terms of microscopic models and theories, they provide information on the forces and interactions at the atomic and molecular level that determine the macroscopic properties.

Thermodynamic Relations

The specific heat of a substance is the amount of heat required to increase the temperature by one degree:

$$C \equiv \frac{\delta q}{\mathrm{d}T}$$

where δq, an inexact differential, is the quantity of heat added and $\mathrm{d}T$ is the increase in temperature produced in the process. By the first law of thermodynamics, $\delta q = \mathrm{d}U - \delta w$, where U is the internal energy and δw is the work done in the process. Since U is a "thermodynamic property," a quantity that depends only on the thermodynamic state of the system, $\mathrm{d}U$ is an exact differential and depends only on the initial and final states. However, δw, and therefore both δq and C, depend on details of the way the process takes place as well as on the initial and final states. If the work is done by an external hydrostatic pressure, P, $\delta w = -P\ \mathrm{d}V$, where V is the volume. In that case,

$$C = \frac{\mathrm{d}U + P\ \mathrm{d}V}{\mathrm{d}T} = \frac{\mathrm{d}(U + PV) - V\ \mathrm{d}P}{\mathrm{d}T}$$

With the definition for the enthalpy, $H \equiv U + PV$, this leads to expressions for the constant volume and constant pressure specific heats,

$$C_V = \left(\frac{\partial U}{\partial T}\right)_V$$

and

$$C_P = \left(\frac{\partial H}{\partial T}\right)_P$$

thermodynamic properties, which can be expressed in, for example, units of $\mathrm{J\,K^{-1}\,mol^{-1}}$. If work is done by magnetic or electric forces, the relevant variables are the magnetic induction, $\boldsymbol{B}$, the magnetization, $\boldsymbol{M}$, the electric field, $\boldsymbol{E}$, and the dielectric displacement, $\boldsymbol{D}$. (In free space $\boldsymbol{B} = \mu_0 \boldsymbol{H}$, where μ_0 is the permeability of free space and $\boldsymbol{H}$ is the magnetic field.) The expressions for the work are $\delta w = \boldsymbol{H}\ \mathrm{d}\boldsymbol{M}$ and $\delta w = \boldsymbol{E}\ \mathrm{d}\boldsymbol{D}$, respectively. In other thermodynamic relations, $\boldsymbol{H}$ or $\boldsymbol{E}$ replaces the intensive variable P and $-\boldsymbol{M}$ or $-\boldsymbol{D}$ replaces the extensive variable V.

With other thermodynamic relations, based on both the first and second laws, it can be shown that

$$C_P - C_V = \frac{TV\alpha^2}{\kappa}$$

where $\alpha = V^{-1}(\partial V/\partial T)_P$ is the thermal expansion, and $\kappa = V^{-1}(\partial V/\partial P)_T$ is the isothermal compressibility. Thermodynamic stability requires that both C_V and κ be positive. Although α can be either positive or negative, it appears as the square, and $C_P - C_V$ is always positive: when the heat is absorbed at constant volume, $\delta w = 0$. In the constant-pressure process there is, generally, a change in V, $\delta w \neq 0$ and can be either positive or negative, but the increase in U ensures that the heat absorbed is always greater than in the constant-volume process. Evaluation of α and κ for an ideal gas, for which $PV = RT$, where R is the gas constant, gives $C_P - C_V = R$.

Microscopic Interpretation

Classical, High-Temperature Limit

In classical statistical mechanics, each term in the Hamiltonian for the total energy that is the square of either a momentum or a coordinate, contributes $(\mathrm{l}/2)k_\mathrm{B}T$ to the thermal energy, where k_B is the Boltzmann constant. For a particle moving freely in space, the translational kinetic energy includes three terms in the square of a momentum, corresponding to the three dimensions in space: $U = (3/2)k_\mathrm{B}T$, and $C_V = (3/2)k_\mathrm{B}$. For Avagadro's number, N_A, of such particles, one mole of an "ideal gas," $C_V = N_A(3/2)k_\mathrm{B} = (3/2)R$. For a particle bound by harmonic forces to a lattice site in three dimensions, there are three terms in the square of a momentum in the kinetic energy and three in the square of a coordinate in the potential energy: $U = 3k_\mathrm{B}T$, and $C_V = 3k_\mathrm{B}$. At sufficiently high temperatures, quantum statistical mechanics gives the same results, the classical or high-temperature limit. At temperatures for which $k_\mathrm{B}T$ is of the order of, or smaller than, the spacing of the quantum mechanically allowed energy levels, the higher energy levels are not fully accessible, and U and C do not reach the classical limit. The energies of the allowed translational states of the particles of an ideal gas are proportional to $m^{-1/2}\,V^{2/3}$, where m is the mass of the particles and V is the volume of the container. For gases of atoms and molecules at ordinary densities, the energy levels are so closely spaced that the classical limit applies at all temperatures of interest, but for an electron gas at densities of the conduction electrons in a metal, that limit is reached only at temperatures $\sim 10^5\,\mathrm{K}$. The specific heat of a harmonic oscillator offers a typical

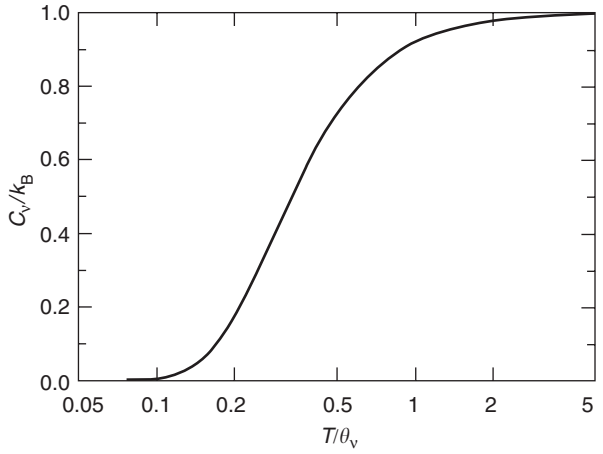

Figure 1 The contribution to the specific heat of a one-dimensional harmonic oscillator, C_v, displayed as C_v/k_B, vs. T/θ_v.

example of the effects of quantization: the energy levels are equally spaced, at intervals of $\hbar\omega \equiv k_B\theta_v$, where $\hbar$ is Planck's constant divided by 2π, T is the characteristic frequency, and θ_v is a defined characteristic temperature. As shown in **Figure 1**, the specific heat approaches k_B in the high-temperature limit and goes to zero, as $\exp(-\theta_v/T)$ at temperatures for which k_BT is less than the energy of the first excited level.

Gases

The heat capacities of gases are often treated in the ideal-gas, rigid-rotor, harmonic-oscillator approximation, in which C is the sum of contributions, C_t, C_r, and C_v, associated with translational, rotational, and vibrational motion, respectively. At sufficiently high temperatures, excited electronic states can also contribute to C_V. For a molecule with n atoms, $3n$ coordinates are required to specify the positions of the atoms: there are $3n$ "degrees of freedom." Three of these are associated with translation of the molecule as a whole; three are associated with rotation for nonlinear molecules, but only two for linear molecules (there is no rotation about the axis); the rest, $3n-6$ or $3n-5$, respectively, are associated with vibration. Each translational degree of freedom contributes one square term to the kinetic energy; each rotational degree of freedom contributes one square term, in an angular momentum, to the kinetic energy; each vibrational degree of freedom contributes one square term to the kinetic energy and one to the potential energy. In the high-temperature limit, and for one mole of gas, $C_v = 3nR$ for nonlinear molecules, but $(3n+1/2)R$ for linear molecules. The vibrational contributions decrease to zero at temperatures below the characteristic temperatures θ_v, as shown in **Figure 1**. The rotational contributions go to zero below characteristic temperatures θ_r that are defined by the allowed rotational energy levels, but there is no general expression for C_r in closed form. Some representative values of θ_v and θ_r are given in **Table 1**. **Figure 2** shows the temperature dependence of C_V for HD, an asymmetric, linear, diatomic molecule. The local maximum near 50 K is related to details of the spacing and degeneracy of the rotational levels. For symmetric molecules, certain combinations of rotational and nuclear spin states are not

Table 1 Characteristic temperatures associated with the vibrational and rotational specific heats of some diatomic molecules and one linear, symmetric, triatomic molecule, CO_2

Molecule	θ_v(K)	θ_v(K)[a]
H_2	6332	88
D_2	4487	43.8
HD	5500	66
HF	5955	30.2
HCl	4304	15.2
HBr	3812	12.2
HI	3321	9.4
N_2	3393	2.88
O_2	2274	2.08
F_2	1283	1.27
Cl_2	805	0.351
Br_2	463	0.116
CO	3122	2.78
NO	2719	2.45
CO_2	3380[b]	1.13
	1928[c]	
	960[d]	

[a] All θ_r are doubly degenerate.
[b] Antisymmetric stretch.
[c] Symmetric stretch.
[d] Perpendicular bending (doubly degenerate).

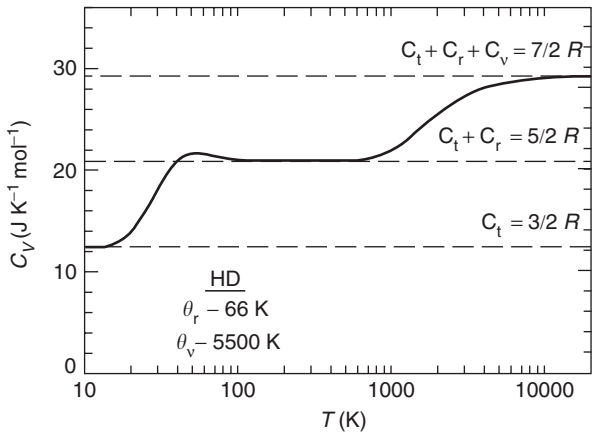

Figure 2 The specific heat at constant volume, C_V, of HD gas. C_V is the sum of translational, rotational, and vibrational contributions, C_t, C_r, and C_v, respectively. The horizontal dashed lines mark the high-temperature limits of the different contributions. (The rotational contribution was obtained from tabulations in: Mayer JE and Mayer MG (1940) *Statistical Mechanics*, p. 450. New York: Wiley.)

allowed. The prototypical examples are o-H_2, with triplet spin and even rotational states, and p-H_2, with singlet spin and odd rotational states. Depending on conditions, transitions between the two spin states can be very slow; o-H_2 and p-H_2 can exist as separate molecules with very different specific heats.

Condensed Matter

Separability of contributions The specific heat of a condensed matter phase is usually taken to be the sum of contributions arising from different modes of excitation. For a nonmagnetic metal these are the lattice, C_l, and electron, C_e, contributions that are associated with, respectively, the vibrational states of the ions that form the lattice and the energy states of the conduction electrons. The vibrational states of the lattice and the energy states of the electrons are not independent, however: The frequencies of the normal modes of the lattice are affected by the presence of the conduction electrons, and the allowed energy states of the electrons are affected by the spatially periodic potential of positive ions of the lattice and also by interaction with the quanta of vibrational energy of the lattice, the phonons. Nevertheless, to an adequate degree of approximation for most purposes, the specific heat can be taken to be the sum of separable contributions from the lattice and the conduction electrons, with the understanding that the energy levels of each system are determined in part by interaction with the other. In experimental data, the two contributions are generally separated by assigning them different, theoretically expected temperature dependences. Similar considerations apply to magnetic contributions, C_m, associated with electronic magnetic moments, and hyperfine contributions, C_h, associated with nuclear moments.

Phonon contribution For one mole of a "monatomic" solid, which has one atom per primitive cell, there are $3N_A$ vibrational degrees of freedom. In the harmonic-lattice approximation, the phonon or lattice contribution to the specific heat, C_l, is the sum of $3N_A$ harmonic-oscillator contributions, one for each of the normal vibrational modes. In the high-temperature limit, also called the Dulong–Petit limit in this context, each contributes k_B to C_l, giving $C_l = 3R$. Anharmonic effects make a contribution to C_l that becomes more important at high temperatures, and can give values of C_l that exceed the Dulong–Petit limit.

In the Einstein model, the normal modes were approximated by $3N_A$ harmonic oscillators with the same frequency, ω_E, corresponding to the characteristic, Einstein temperature, $\Theta_E \equiv \hbar\omega_E/k_B$. The Einstein expression for the specific heat is

$$\frac{C_E}{3R} = \left(\frac{\Theta_E}{T}\right)^2 \frac{\exp(\Theta_E/T)}{[\exp(\Theta_E/T) - 1]^2}$$

This model is of historical importance because it was the first to account for the decrease of C_l at low temperature, but it gives $C_l \propto \exp(-\Theta_E/T)$ in the low-temperature limit, while the experimentally observed behavior is $C_l \propto T^3$.

In the Debye model, the frequencies of the normal modes were approximated by those of the acoustic modes in an elastic continuum. A cutoff frequency, ω_D, was introduced to limit the number of modes to $3N_A$. The cutoff frequency, and the Debye temperature, $\Theta_D \equiv \hbar\omega_D/k_B$, can be calculated from the elastic constants. The Debye specific heat, given by an integral over the phonon density of states,

$$\frac{C_D}{3R} = 3\left(\frac{T}{\Theta_D}\right)^3 \int_0^{\Theta_D/T} \frac{x^4 e^x}{(e^x - 1)^2}\, dx$$

is a function of T/Θ_D. In the low-temperature limit, $C_D = (12/5)\pi^4 R(T/\Theta_D)^3$, in agreement with experiment with respect to both the T^3 temperature dependence and the relation of Θ_D to the elastic constants. **Figure 3** is a comparison of the Debye model with the lattice specific heat of Cu. The best fit to the data for $10 \leqslant T \leqslant 300$ K is obtained with

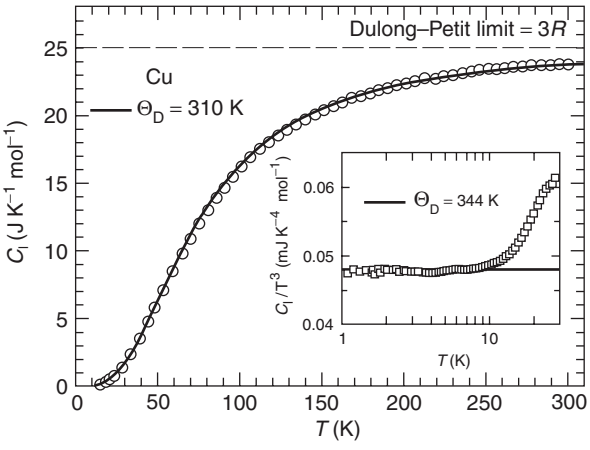

Figure 3 The lattice specific heat, C_l, of Cu: compared with the Debye model for $10 \leqslant T \leqslant 300$ K in the main panel; compared with the low-temperature, T^3 behavior predicted by the Debye model in the inset. The electron contribution to C_V has been subtracted to obtain C_l as plotted here. The data for the main panel are from: Giauque WF and Meads PF (1941) The heat capacities and entropies of aluminum and copper from 15 to 300 K. *Journal of the American Chemical Society* 63: 1897. The measurements were made at constant pressure, but corrected to C_V with the values of α and κ. (The low-temperature data in the inset are from measurements (unpublished) made in the authors' laboratory at the University of California, Berkeley, California 94720, USA.)

$\Theta_D = 310$ K, but the data in the low-temperature, T^3 region gives $\Theta_D = 344$ K, in agreement with the value calculated from the elastic constants. This comparison of data for a monatomic metal with the Debye model is fairly typical: at low temperatures, the Debye model gives the T^3 term, the contribution of the lowest-frequency acoustic phonons, correctly. Although the Debye model gives T^3 behavior for $T \leqslant \Theta_D/10$, and negative deviations from T^3 behavior at higher temperatures, experimental data typically show deviations that are positive and occur at lower temperatures. The negative deviations given by the model are a consequence of the sharp cutoff frequency; the positive deviations in a real solid are a consequence of phonon dispersion, which is neglected in the model. At higher temperatures, where the model is an approximation, experimental data cannot be fitted accurately with a single value of Θ_D. The value determined by the "best fit" in some interval of temperature is an average that reflects the structure in the phonon density of states for the real lattice at frequencies that contribute to C_l in that interval. The T^3 phonon contribution to the specific heat is also observed in liquids, as shown in an inset to **Figure 11** for ^{4}He.

Although the Debye model is a useful approximation to the lattice specific heat of many materials over a wide range of temperatures, experimental data can show substantial deviations, particularly at intermediate temperatures. For a discrete lattice with n atoms per primitive unit cell, the frequency distribution of the normal modes is that of three acoustic phonon branches and $3n - 3$ optical phonon branches. For the acoustic branches, phonon dispersion, the variation of the sound velocity with frequency, has an important effect on the phonon density of states that is not taken into account in the Debye model. The optical modes are omitted in this model. The harmonic-lattice approximation, which gives an expansion of C_l in odd powers of T that starts with the Debye T^3 term, is often used to fit experimental data at low temperatures. Sums of Einstein functions, which represent contributions from the optical modes or other peaks in the phonon density of states, and a Debye function are useful over a wide range of intermediate temperatures. **Figure 4** shows an unusual case, C_l for YbGaGe, which is well represented by a single Einstein frequency and a Debye function.

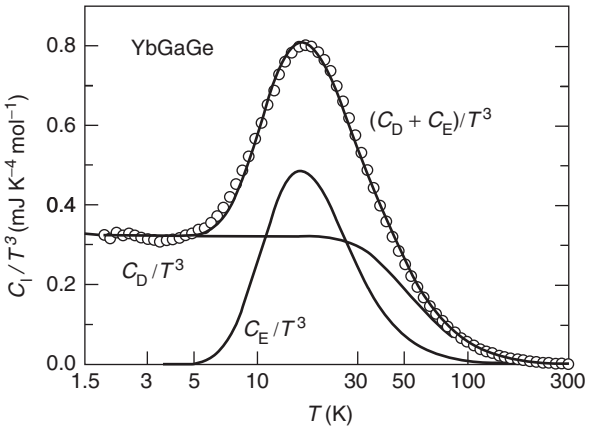

Figure 4 The lattice heat capacity of YbGaGe, as C_l/T^3 vs. log T, fitted with the sum of one Einstein function and one Debye function. The peak in C_l/T^3 centered near 20 K is an unusually prominent, but otherwise typical, signature of a "soft mode," a peak in the phonon density of states. (Specific-heat data are from measurements made at the Los Alamos National Laboratory, Los Alamos, New Mexico: Drymiotis FR, Lawes G, Migliori A, Ledbetter H, Betts JB, *et al.* (2004), unpublished. The electron contribution was subtracted from the data for this figure.)

Conduction electron contribution At ambient and low temperature, and at the densities at which they occur in metals, the conduction electrons must be treated with Fermi–Dirac statistics: there can be at most two electrons, with opposite spin, in any energy state. Their contribution to the specific heat is similar to that of the hypothetical "free electron gas," in which there are no interactions between the electrons or with the lattice. For free electrons, the allowed states have kinetic energies proportional to the sum of the squares of the wave vectors. At $T = 0$, the states are filled up to the Fermi energy,

$$E_F = \left(\frac{\hbar^2}{2m_e}\right)\left(\frac{\pi^2 z N_A}{V}\right)^{2/3}$$

where m_e is the electron mass, z is the "valence," and zN_A the number of electrons in the atomic volume, V. For values of the parameters appropriate to metals, the corresponding characteristic temperature, the Fermi temperature, $T_F \equiv E_F/k_B$, has values $\sim 10^4$–10^5 K. For $T \ll T_F$, most of the states at $E < E_F$ remain fully occupied. It is only electrons with energies within a range $k_B T$ in energy in the vicinity of E_F that can be thermally excited, and by an energy that is also of order $k_B T$. The simple argument that a fraction of the electrons, T/T_F, makes the classical contribution gives $C_e \sim RT/T_F$, which agrees both in temperature dependence and order of magnitude with experimental observations. An exact calculation gives

$$C_e = \left(\frac{\pi^2 z R}{2}\right)\left(\frac{T}{T_F}\right) = \left(\frac{\pi^2 k_B^2}{3}\right) N(E_F) T \equiv \gamma T$$

where $N(E_F)$ is the density of electron states at the Fermi level. The coefficient γ, as defined here for the free electron gas, is proportional to m_e.

The properties of the conduction electrons in a metal are modified by the interactions of the electrons with the periodic potential of the lattice, by electron–electron interactions, and by the electron–phonon interaction. However, according to Landau's Fermi-liquid theory, there is a one-to-one correspondence between excitations in the free electron gas and those in the gas with interactions; the coefficient γ is changed, with m_e replaced with an "effective mass," m^*, but the temperature dependence of C_e is unchanged. The periodic potential of the lattice modifies the relation between electron energy and wave vector. The effect on $N(E_F)$ is to replace m_e with m_{bs}, the "band-structure mass," in the expression for γ. The electron–phonon interaction, which is also responsible for the pairing of the electrons in the BCS theory of superconductivity, introduces an enhancement of γ by a factor $(1+\lambda)$. In many cases m_{bs} can be calculated with good accuracy, and comparisons with experimental values of γ give the values of λ. For most metals, λ is in the range 0.2–1, with higher values occurring for strong-coupled superconductors such as Hg and Pb. (There is also a contribution to m^* from electron–electron interactions, but it is small, difficult to determine, and usually ignored.) The combined effect of the lattice potential and the electron–phonon interaction gives $m^* = (1+\lambda)\, m_{bs}$. Experimental values of m^*/m_e are ~ 1 for many metals, as high as 10 for some transition and lanthanide metals, and 10^2–10^3 for heavy-fermion compounds, mainly Ce and U intermetallic compounds, in which the large effective mass is associated with the Kondo effect.

Many metals undergo a transition to the superconducting state at a critical temperature, T_c. In most cases, the superconducting-state C_e is approximately exponential in temperature as predicted by the BCS theory, but T^2 and T^3 dependences are found in some "unconventional" superconductors, including heavy-fermion and cuprate superconductors. C_e for Al, a BCS superconductor with $T_c = 1.2$ K, is shown for both the superconducting and normal states in **Figure 5**. In this case the lattice contribution to the specific heat at T_c and below is relatively small, and C_e in the superconducting state is particularly well defined by the experimental data.

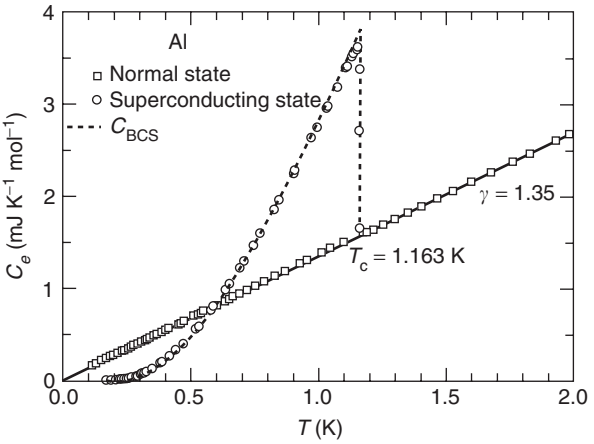

Figure 5 Conduction electron contribution to the specific heats of Al in the normal and superconducting states. The normal-state data below T_c were obtained in a magnetic field that quenched the superconductivity. The dashed curve is the theoretical specific heat of a BCS superconductor (Bardeen J, Cooper LN, and Schriffer JR (1957) Microscopic theory of superconductivity. *Physical Review* 106: 162), with numerical values from: Mühlschlegel B (1959) *Zeitschrift fur physik* 155: 313. Specific-heat data for aluminum are from: Phillips NE (1959) Heat capacity of aluminum between 0.1 and 4.0 K. *Physical Review* 114: 676.

Magnetic contribution Magnetic moments, of the order of magnitude of the Bohr magneton, μ_B, can be associated with the itinerant electrons in a metal and can appear as localized moments in both metals and insulating materials. At sufficiently high temperatures, in the paramagnetic phase, and in the absence of an applied magnetic field, they are randomly oriented and contribute $R\ln(2J+1)$ to the entropy, S, where J is the resultant angular momentum. However, there is always some internal interaction that tends to produce an ordered structure at temperatures for which k_BT is small relative to the energy of the interaction. In both metals and insulators, the possible interactions include dipole–dipole interactions and exchange interactions. In metals, the RKKY interaction that couples the localized moments via an intermediate polarization of the conduction electrons, and the Kondo effect, which leads to a compensation of the localized moments by conduction electron moments, are also important. In accordance with the third law of thermodynamics, the interactions produce a completely ordered, zero-entropy state at $T = 0$. (Possible exceptions are "frustrated" antiferromagnets, in which the exchange interactions cannot all be satisfied simultaneously.) In the temperature region in which the ordering and the associated reduction in entropy occur, there is a "specific-heat anomaly," a peak in the specific heat, which is related to the entropy by $C_P = (\partial S/\partial T)_P$. The temperature at which the ordering occurs can vary widely, reflecting differences in the energies of the interaction, for example, less than 1 mK for $Ce_2Mg_3(NO_3)_{12}\cdot 24H_2O$ and 1043 K for metallic iron.

When the ordering is driven by an external field, there are $2J+1$ states with energies $gm_J\mu_B\boldsymbol{B}$, where g is the spectroscopic splitting factor and m_J takes values from $-J$ to $+J$. The specific heat associated with

the magnetic ordering, C_m, takes the form

$$\frac{C_m}{R} = \left(\frac{g\mu_B \boldsymbol{B}}{2k_B T}\right)^2 \left\{ \operatorname{csch}^2\left(\frac{g\mu_B \boldsymbol{B}}{2k_B T}\right) - (2J+1)^2 \operatorname{csch}^2\left[(2J+1)\left(\frac{g\mu_B \boldsymbol{B}}{2k_B T}\right)\right] \right\}$$

This is an example of a Schottky anomaly, a term that is used more generally for any specific-heat anomaly associated with a finite number of energy levels. Electric fields of the crystal lattice acting on the orbital component of the angular momentum can also split the manifold of $2J+1$ states of the isolated ion to produce a Schottky anomaly, in that case called a crystal-field anomaly. For an external magnetic field and $J = 1/2$, an example of a "two-level system," the anomaly takes a particularly simple form,

$$\frac{C_m}{R} = \left(\frac{\Delta}{k_B T}\right)^2 \frac{\exp(\Delta/k_B T)}{[1+\exp(\Delta/k_B T)]^2}$$

where Δ is the energy difference between the two states, in this case $g\mu_B \boldsymbol{B}$. $CuK_2(SO_4)_2 \cdot 6H_2O$ in a field of 1.5 T provides an example of this behavior: the internal interactions, which produce an ordering near 0.05 K in the absence of an external field, can be neglected and the experimental data are in good agreement with the calculated two-level Schottky anomaly, as shown in **Figure 6**.

The internal interactions in α-$MnCl_2 \cdot 4H_2O$ produce antiferromagnetic ordering that results in a specific-heat anomaly near 1.5 K. **Figure 7** shows the zero-field anomaly, which has a shape typical of that associated with ordering by exchange interactions, and the evolution of the anomaly to a more Schottky-like form in an increasing external field. **Figure 8** shows the specific heat of $CeCu_6$, a heavy-fermion compound, in the low-temperature region where the Kondo effect produces a compensation of the Ce moments by an exchange interaction with the conduction electrons.

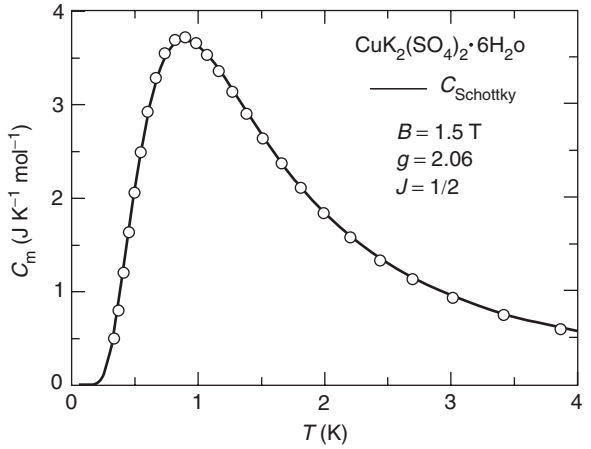

Figure 6 The magnetic specific heat, C_m, of $CuK_2(SO_4)_2 \cdot 6H_2O$ in a magnetic field of 1.5 T. At the temperatures of the measurements, the interactions between the magnetic Cu^{2+} ions have a negligible effect, and a "two-level" Schottky function for isolated ions provides an excellent fit to the data. (The data are from: Giauque WF, Brodale GE, Hornung EW, and Fisher RA (1971) Magnetothermodynamics of $CuK_2(SO_4)_2 \cdot 6H_2O$. II. Magnetic moment, heat capacity, entropy from 0.5 to 4.2 K with fields to 90 kG along the γ magnetic axis. *Journal of Chemical Physics* 54: 273.)

Nuclear moment contribution Contributions to the specific heat associated with nuclear moments, the "hyperfine" specific heat, C_h, are analogous to those associated with electronic moments. The differences arise from the small size of the nuclear magnetic moments, of the order of magnitude of the nuclear magneton, μ_N, three orders of magnitude smaller than μ_B, and the existence of nuclear electric quadrupole moments, Q, which interact with electric-field gradients in the lattice. The nuclear magnetic moments interact with external applied magnetic fields and with internal hyperfine fields produced by ordered electronic moments. They interact with each other through direct dipole–dipole interactions and, in the case of metals, through RKKY coupling. Except in the case of the internal hyperfine fields, which can be very large, it is generally only the high-temperature tail of a Schottky anomaly, associated with the interactions with magnetic fields or electric-field gradients, that is observed. For the case that the electric-field gradient and the magnetic field are in the same direction, the first two terms in the high-temperature expansion of the Schottky anomaly for C_h are D_2/T^2 and D_3/T^3, the coefficients of which have the forms

$$\frac{D_2}{R} = \left(\frac{1}{80}\right)\left[\frac{(I+1)(2I+3)}{I(2I-1)}\right]\left(\frac{e^2qQ}{k_B}\right)^2 + \left(\frac{1}{3}\right)\left(\frac{I+1}{I}\right)\left(\frac{\mu \boldsymbol{B}}{k_B}\right)^2$$

and

$$\frac{D_3}{R} = -\left(\frac{1}{1120}\right)\left[\frac{(2I-3)(I+1)(2I+3)(2I+5)}{2I^2(2I-1)^2}\right] \times \left(\frac{e^2qQ}{k_B}\right)^3 - \left(\frac{1}{10}\right)\left[\frac{(I+1)(2I+3)}{2I^2}\right] \times \left(\frac{e^2qQ}{k_B}\right)\left(\frac{\mu \boldsymbol{B}}{k_B}\right)^2$$

where I is the nuclear spin, μ is the nuclear moment in units of μ_N, e^2q is the electric field gradient, and Q is the nuclear quadrupole moment. These terms have

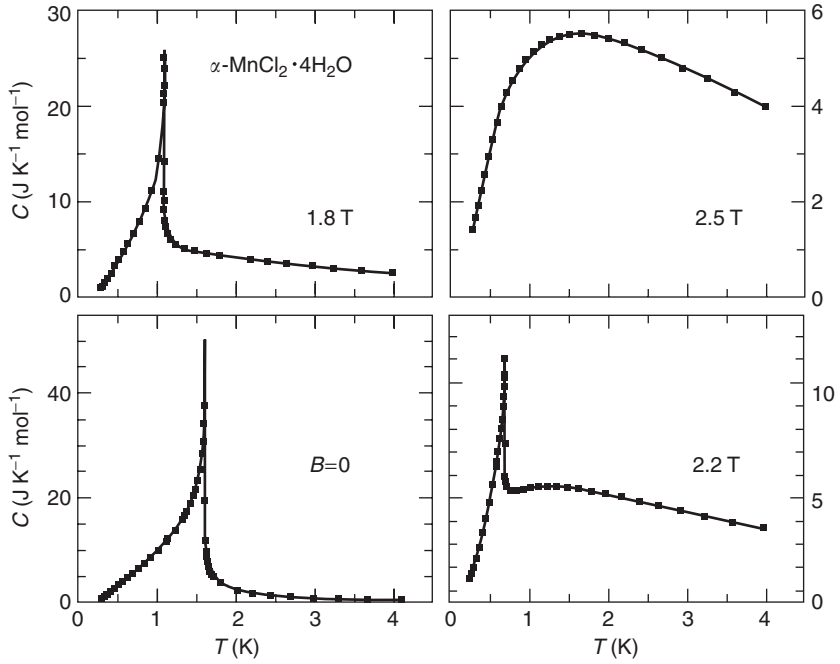

Figure 7 Specific heats for α-$MnCl_2 \cdot 4H_2O$ in various magnetic fields. For $\boldsymbol{B} = 0$, the Mn^{2+} ions order antiferromagnetically with a "lambda" anomaly at a Néel temperature of 1.6 K. As the magnetic field is increased, the antiferromagnetic ordering moves to lower temperatures and the anomaly is attenuated. For sufficiently large $\boldsymbol{B}$, the antiferromagnetic ordering is suppressed and the specific heat evolves into a more Schottky-like anomaly. (The data are from: Giauque WF, Fisher RA, Brodale GE, and Hornung EW (1970) Magnetothermodynamics of α-$MnCl_2 \cdot 4H_2O$. II. Heat capacity, entropy, magnetic moment from 0.4 to 4.2 K with fields to 90 kG along the *b* crystallographic axis. *Journal of Chemical Physics* 52: 2901.)

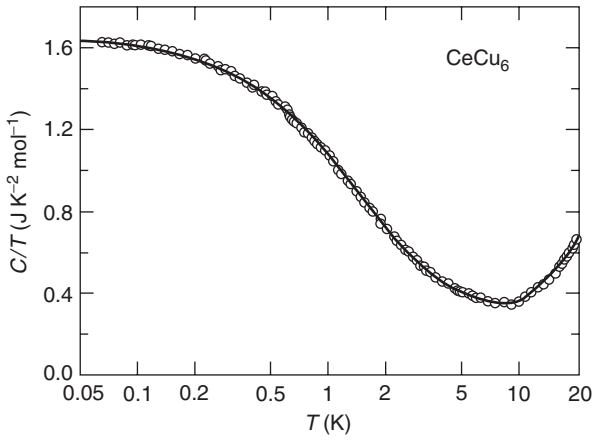

Figure 8 *C*/*T* vs. log *T* for the heavy-fermion compound $CeCu_6$. The high values of the heat capacity at temperatures below 5 K are a manifestation of the Kondo effect, in which the exchange interaction between the localized 4*f* moments of the Ce ions and the conduction electrons produces a compensation of the Ce moments by the conduction electrons. The associated specific heat is described by a temperature-dependent coefficient of the electron specific heat, $\gamma(T)$. At $T = 0.064$ K, $\gamma(T)$ has increased to $1.63\,J\,K^{-2}\,mol^{-1}$, corresponding to a conduction electron effective mass, m^*, that is three orders of magnitude greater than the free electron mass. (The data are from: Fisher RA, Lacy SE, Marcenat C, Olsen JA, Phillips NE, *et al.* (1987) Specific heat of heavy-fermion $CeCu_6$: effect of pressure and magnetic field. *Journal of Applied Physics* (*Japan*) 26: 1257.)

been identified in experimental data, usually in the vicinity of 0.1–1 K. The large internal hyperfine field, 930 T, in Ho, produces a Schottky anomaly with a maximum near 0.3 K. **Figure 9** is a comparison of the experimental data with the fitted Schottky anomaly, which includes a small quadrupole contribution. Examples of nuclear ordering at the other extreme of the temperature range in which the phenomenon is known are provided by Cu and Ag: in both cases the nuclei order antiferromagnetically, by a combination of dipole–dipole and RKKY interactions, and reductions in the nuclear entropy related to the associated specific-heat anomaly have been observed experimentally. The ordering occurs in the vicinity of 50 nK for Cu, and in the vicinity of 0.8 nK for Ag, which has a lower concentration of nuclear magnetic moments that are also smaller in magnitude.

Phase transitions Phase transitions take a variety of forms and display a corresponding variety in the associated specific-heat anomalies. Discontinuities in the entropy and the volume, the first derivatives of the Gibbs energy, *G*, are the defining characteristic of a thermodynamic first-order transition. They are related to the slope of the phase boundary in the *P*–*T* plane

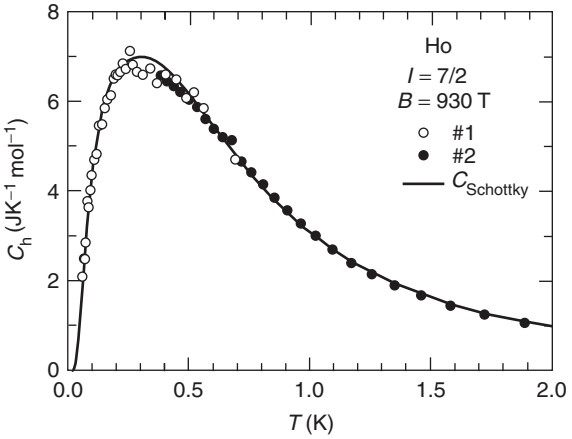

Figure 9 The hyperfine specific heat, C_h, for two samples of ferromagnetically ordered Ho metal. The splitting of the nuclear spin states arises mainly from the interaction of the nuclear magnetic moments with the effective hyperfine field created by the ordered 4*f* electron moments, but there is also a small effect of interaction of the electric quadrupole moment with an electric field gradient. The solid curve, a theoretical fit to the data, is a Schottky function calculated for the resulting, unevenly spaced levels. (The data for sample ♯1 are from: Van Kampen H, Miedema AR, and Huiskamp WJ (1964) Heat capacities of the metals terbium and holmium below 1 K. *Physica* 30: 229; for sample ♯2, from: Lounasmaa OV (1962) Specific heat of holmium metal between 0.38 and 4.2 K. *Physical Review* 128: 1136.)

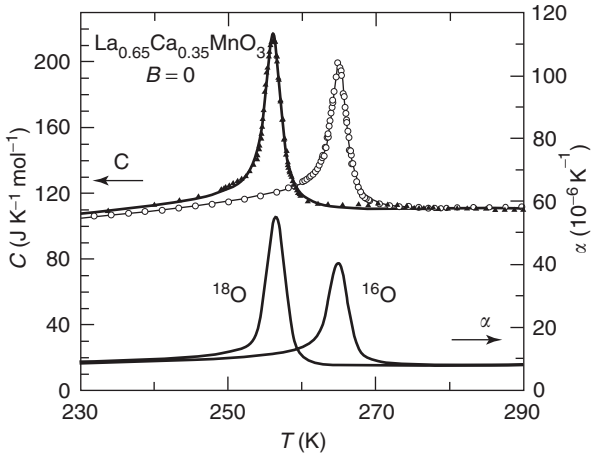

Figure 10 The specific heat, *C*, and thermal expansion, α, of $La_{0.65}Ca_{0.35}MnO_3$, a "colossal magnetoresistance" material that undergoes a first-order transition from a high-temperature, insulating, paramagnetic phase to a low-temperature, metallic, ferromagnetic phase. The transition, at the Curie temperature, shows a strong isotope effect. Data for both ^{16}O and ^{18}O samples are shown. (The data are from: Gordon JE, Marcenat C, Franck JP, Isaac I, Zhang G, *et al.* (2001) Specific heat and thermal expansion of $La_{0.65}Ca_{0.35}MnO_3$: magnetic-field dependence, isotopic effect, and evidence for a first-order phase transition. *Physical Review B* 65: 24441.)

by the Clapeyron equation, $dP/dT = \Delta S/\Delta V$. Ideally, there would be a δ function in *C* at the transition that would integrate to $T\Delta S$, but the transition is usually broadened by impurities, inhomogeneity, or other factors. **Figure 10** shows the specific heat at the first-order transition associated with the ferromagnetic ordering in $La_{0.65}Ca_{0.35}MnO_3$. In that case, the random mixture of La and Ca ions on their common sites accounts quantitatively for the breadth of the transition. The fitted curves correspond to broadened discontinuities in the entropy and the specific heat. The thermal-expansion data, included in the same figure, illustrate the similarity in the temperature dependence of the two properties, which is expected on the basis of simple thermodynamic models. They also give the value of ΔV, which, together with ΔS from the specific-heat data, satisfies the Clapeyron equation, confirming the first-order nature of the transition.

At an Ehrenfest second-order transition, the first derivatives of the Gibbs energy are continuous, but there are discontinuities in the second derivatives, the specific heat, the thermal expansion, and the compressibility. The Ehrenfest relations for the slope of the phase boundary are $dP/dT = \Delta\alpha/\Delta\kappa = \Delta C_P/\Delta VT\Delta\alpha$. The zero-field transition of a metal from the normal state to the superconducting state is an Ehrenfest second-order transition with a discontinuity between two finite values of the specific heat. The transition in Al, shown in **Figure 5**, is an example. For many second-order transitions, the specific heat diverges at the transition, as illustrated by the antiferromagnetic ordering in α-$MnCl_2 \cdot 4H_2O$ in **Figure 7**. They are frequently called λ transitions, as suggested by the shape of the specific-heat anomaly and the name given to the transition to the superfluid state in liquid ^{4}He at the "λ point." The λ transition in ^{4}He, for which the specific heat is shown in **Figure 11**, has been particularly intensively studied because an exceptionally high degree of sample purity and homogeneity can be attained. In the vicinity of the λ point, the specific heat varies as $\ln|T - T_\lambda|$.

Thermodynamics of Chemical Reactions

Currently, most measurements of specific heat are made for the interest in their microscopic interpretation, but historically a major motivation was to obtain data relevant to the third law of thermodynamics and to the thermodynamics of chemical reactions more generally. At constant pressure and temperature, the conditions for equilibrium between the products and reactants of a chemical reaction, and for equilibrium between two phases of the same substance, are determined by the change in Gibbs energy for the transformation. At constant volume and temperature, the change in the Helmholtz energy, *A*, takes that role. Specific-heat data contribute to the determination of

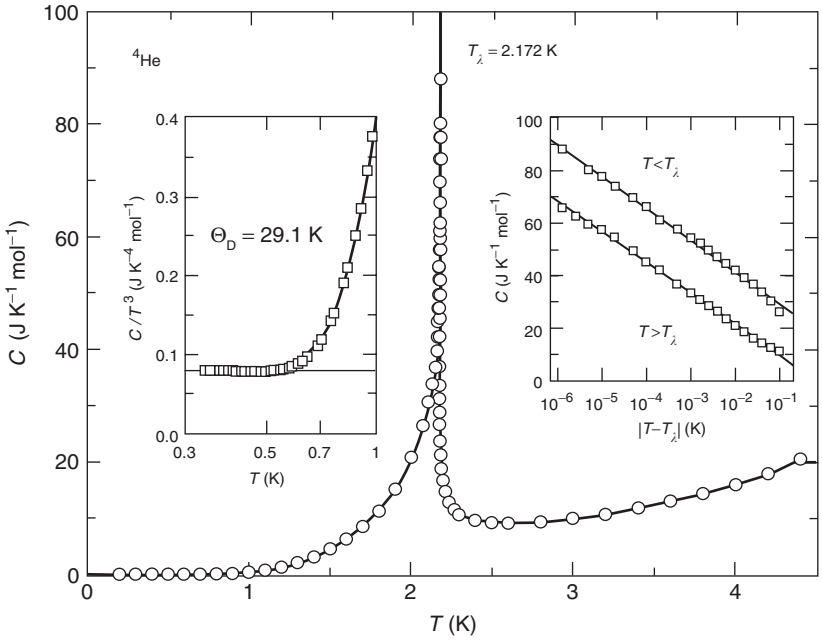

Figure 11 The specific heat of liquid ^{4}He. At T_λ, there is a transition from a low-temperature superfluid phase to a high-temperature, normal-liquid phase. The superfluid phase has properties that are analogous to those of a metal in the superconducting state. As shown in the inset on the left, $C \propto T^3$ for $T \leqslant 0.5$ K: The phonon contribution to the specific heat has the same form, and the same relation to elastic constants, as in solids. In this case, the initial deviation from the T^3 dependence includes a "roton" contribution. At T_λ, there is a logarithmetic divergence of the specific heat, as demonstrated in the inset on the right. (The data for the main panel and right inset are from: Buckingham MJ and Fairbanks WK (1961) The nature of the λ-transition in liquid helium. In: Gorter CJ (ed.) *Progress in Low Temperature Physics*, vol. 3. Amsterdam: North-Holland; for the left inset, from: Hoffer JK (1968) *PhD Thesis* (unpublished), Lawrence Berkeley National Laboratory, University of California, Berkeley, California 94720, USA.)

the Gibbs and Helmholtz energies through the thermodynamic relations $G \equiv H - TS$, $(\partial H/\partial T)_P = C_P$, $(\partial S/\partial T)_P = C_P/T$, $A \equiv U - TS$, $(\partial U/\partial T)_V = C_V$, and $(\partial S/\partial T)_V = C_V/T$. They determine the values of the entropy, and the temperature dependences of the enthalpy, energy, and Gibbs and Helmholtz energies.

As stated in one of the many formulations of the third law of thermodynamics, for any substance in a perfect crystalline state, the entropy is zero in the limit $T \to 0$. The importance for chemical thermodynamics is that values of the entropy can be obtained from specific-heat data alone: the "third-law entropy" is obtained by extrapolating specific-heat data to 0 K, integrating C_P/T to obtain $S(T)$–S_0, and assuming, as suggested by the third law, that S_0, the entropy at the 0 K state reached by the extrapolation, is zero. Typically, the data extend to a temperature between 1 and 15 K, the extrapolation is by a semi-empirical fit to the lowest-temperature data that is based on appropriate theoretical expressions, and the entropies are tabulated for 298.15 K and the standard state (the thermodynamically stable form of the substance at a pressure of one bar).

The agreement obtained in comparisons of the values of ΔS for chemical reactions calculated with and without using third-law entropies, and in comparisons of the third-law entropies with values calculated from spectroscopic data played an important role in establishing the third law. In other cases, however, similar comparisons led to the identification of substances, for example, CO, NO, and H_2O, that do not attain a "perfect crystalline state" at 0 K, and for which $S_0 \neq 0$. The existence of such materials emphasizes the importance of caution in applying the third law to the determination of entropies from specific-heat data. The third law of thermodynamics, unlike the first and second laws, cannot be expressed by a simple mathematical relation that applies rigorously in all cases. Its application requires an understanding of its nature, which can be based on a statistical mechanical expression for the entropy, the Boltzmann formula, $S = k_B \ln \Omega$ (where Ω is the number of accessible quantum states, subject to the constraint of a fixed energy), together with the principle that there is a single state of lowest energy that is reached at $T = 0$ by systems that are in thermodynamic equilibrium. The case of CO, which is well understood, is a useful illustration of the factors that determine whether or not $S_0 = 0$: In the solid, the two orientations of a molecule that differ by an interchange of the C and O atoms are two distinguishable states, but, because the molecule is

relatively symmetric with respect to both shape and electric charge distribution, the difference in energy is small. The lowest energy configuration is one in which there is a perfectly ordered arrangement of the molecules with each in a definite orientation relative to the others, but the energy is not much lower than that of the higher-entropy, random distribution of orientations that is thermodynamically stable at high temperature. Below $\sim 5\,\mathrm{K}$ the lower-energy, ordered configuration does become thermodynamically stable, but there is a potential barrier to reorientation of the molecules that exceeds the thermal energy at that temperature, and the perfectly ordered state is not attained. For kinetic reasons, there is "frozen-in disorder" at 0 K and $S_0 \neq 0$. In the completely random configuration, there are two possible states for each molecule, $\Omega = 2^{N_A}$, $S = R \ln 2 = 5.76\,\mathrm{J\,K^{-1}\,mol^{-1}}$. The experimental value is $S_0 = 4.2\,\mathrm{J\,K^{-1}\,mol^{-1}}$, indicating that the molecules are partially ordered, at least in the particular measurement that gave this result. There are other cases, for example, NO, H_2O, and the H_2O in $Na_2SO_4 \cdot 10H_2O$, in which the disorder is complete. These examples afford an understanding of the treatment of nuclear contributions to the entropy: the random distribution over the lattice sites of different isotopes of the same element persists to 0 K, the disorder is frozen-in, and there is no contribution to experimental specific-heat data. The disorder associated with nuclear spin orientation is not frozen in, but at temperatures above 1 K it is normally complete, the associated entropy is constant, and there is no contribution to the specific heat. Both of these contributions to the entropy cancel in chemical reactions, and, although they could be calculated with the Boltzmann formula, they are omitted in tabulations of the entropies of chemical substances. There are also some paramagnetic salts in which the magnet moments of the unpaired electrons, as in the case of nuclear moments, order only below 1 K. Specific-heat measurements to 1 K would suggest $S_0 \neq 0$, but measurements to sufficiently low temperature would give $S_0 = 0$.

The enthalpy, energy, and Gibbs and Helmholtz energies cannot be determined from specific-heat data alone. Tabulations of thermodynamic data give the values of these quantities for compounds in their standard states, relative to the values for the elements in their standard states, for example, as values of the "heat of formation," ΔH, for the reaction in which the compound is formed from the elements. Specific-heat data do determine the temperature dependences of these quantities, but determination of absolute values requires, in addition, the evaluation of constants of integration. For the enthalpy and energy, one constant of integration is needed, for example, one value of a heat of formation for the enthalpy; for the Gibbs and Helmholtz energies, two are needed.

See also: Bose–Einstein Condensation; Diffusionless Transformations; Incommensurate Phases; Irreversible Thermodynamics and Basic Transport Theory in Solids; Phase Transformation; Phase Transformations, Mathematical Aspects of; Phases and Phase Equilibrium; Thermodynamic Properties, General.

PACS: 51.30.+i; 63.20.−e; 65.40.Ba; 65.40.De; 65.40.Gr; 67.40.Kh; 74.25.Bt; 75.20.Hr; 75.20.−g; 75.40.Cx; 75.50.Cc; 75.50.Ee; 82.60.Fa; 75.20.Hr

Further Reading

Ashcroft NW and Mermin ND (1976) *Solid State Physics*. New York: Holt, Rinehart and Winston.

Atkins P and de Paula J (2002) *Physical Chemistry*, 7th edn. New York: W. H. Freeman.

Barron THK and White GK (1999) *Heat Capacity and Thermal Expansion at Low Temperatures*. New York: Kluwer.

Blackman M (1955) In: Flügge S (ed.) *Encyclopedia of Physics*, vol. 7, part 1, p. 325. Berlin: Springer.

Callen HB (1963) *Thermodynamics*. New York: Wiley.

Davidson N (1962) *Statistical Thermodynamics*. New York: McGraw-Hill.

Giauque WF (1969) *The Scientific Papers of William F. Giauque, Low Temperature, Chemical, and Magnetothermodynamics*, vol. 1. New York: Dover.

Giauque WF (1995) *The Scientific Papers of William F. Giauque, Low Temperature, Chemical, and Magnetothermodynamics*, vols. 2 and 3. Berkeley, California: University of California Printing Services.

Gopal ESJ (1966) *Specific Heats at Low Temperatures*. New York: Plenum.

de Jongh LJ and Miedema AR (1974) *Experiments on Simple Magnetic Model Systems*. London: Taylor and Francis.

Kittel C (1963) *Quantum Theory of Solids*. New York: Wiley.

Kittel C (1986) *Introduction to Solid State Physics*, 6th edn. New York: Wiley.

Kittel C and Kroemer H (1989) *Thermal Physics*, 2nd edn. New York: W. H. Freeman.

de Launay J (1956) The theory of specific heats and lattice vibrations. In: Seitz F and Turnbull D (eds.) *Solid State Physics*, vol. 2, p. 219. New York: Academic press.

Phillips NE (1971) Low-temperature heat capacity of metals. *CRC Critical Reviews in Solid State Sciences*, vol. 467. New York: CRC Press.

Pitzer KS (1995) Thermodynamics, 3rd edn., vol. 2. New York: McGraw-Hill.

Nomenclature

A	Helmholtz energy ($\mathrm{J\,mol^{-1}}$)
B	magnetic induction (T) (tesla ≡ weber $\mathrm{m^{-2}}$)
B_h	hyperfine magnetic induction (T)
C	specific heat ($\mathrm{J\,K^{-1}\,mol^{-1}}$)
C_e	electronic specific heat ($\mathrm{J\,K^{-1}\,mol^{-1}}$)
C_h	hyperfine specific heat ($\mathrm{J\,K^{-1}\,mol^{-1}}$)
C_l	lattice specific heat ($\mathrm{J\,K^{-1}\,mol^{-1}}$)

C_m	magnetic specific heat ($J K^{-1} mol^{-1}$)
C_P	specific heat at constant pressure ($J K^{-1} mol^{-1}$)
C_r	rotational specific heat ($J K^{-1} mol^{-1}$)
C_t	translational specific heat ($J K^{-1} mol^{-1}$)
C_v	vibrational specific heat ($J K^{-1} mol^{-1}$)
C_{BCS}	specific heat of a BCS superconductor ($J K^{-1} mol^{-1}$)
C_D	Debye specific heat ($J K^{-1} mol^{-1}$)
C_E	Einstein specific heat ($J K^{-1} mol^{-1}$)
C_V	specific heat at constant volume ($J K^{-1} mol^{-1}$)
D	electric displacement vector ($C m^{-1}$ (coulomb m^{-1}))
e	electron charge (C (coulomb))
e^2q	electric-field gradient at the nucleus ($V m^{-2}$ (volt m^{-2}))
E	electric field ($V m^{-1}$ (volt m^{-1}))
E_F	Fermi energy ($J mol^{-1}$)
g	spectroscopic splitting factor (dimensionless)
G	Gibbs energy ($J mol^{-1}$)
$\boldsymbol{H}$	magnetic field ($A m^{-1}$ (ampere m^{-1}))
H	enthalpy ($J mol^{-1}$)
I	nuclear spin quantum number (dimensionless)
J	electronic spin quantum number (dimensionless)
k_B	Boltzmann constant ($J K^{-1}$)
m	mass (kg)
m_e	free electron mass (kg)
m_J	quantum numbers labeling sublevels of J in a magnetic field (dimensionless)
m_{bs}	electron mass from band structure calculations (kg)
m^*	effective electron mass (kg)
$\boldsymbol{M}$	magnetic moment ($J T^{-1} mol^{-1}$)
n	number of atoms (dimensionless)
N_A	Avagadro's number (mol^{-1})
$N(E_F)$	density of states at the Fermi energy (states $J^{-1} mol^{-1}$)
P	pressure ($N m^{-2}$ (newton m^{-2} = pascal))
q	heat ($J mol^{-1}$)
Q	nuclear electric quadrupole moment (m^2)
R	gas constant ($J K^{-1} mol^{-1}$)
S	entropy ($J K^{-1} mol^{-1}$)
T	temperature (K)
T_c	superconducting critical temperature (K)
T_F	Fermi temperature (K)
T_λ	lambda temperature for ^{4}He superfluid transition (K)
U, E	energy ($J mol^{-1}$)
V	volume (m^3)
w	work ($J mol^{-1}$)
z	valence (dimensionless)
α	thermal expansion (K^{-1})
Δ	energy difference between two states (J)
γ	Sommerfeld constant ($J K^{-2} mol^{-1}$)
θ_r	characteristic rotation temperature (K)
θ_v	characteristic vibration temperature (K)
Θ_D	Debye temperature (K)
Θ_E	Einstein temperature (K)
κ	isothermal compressibility ($m^{-2} kg^{-1}$)
λ	electron–phonon interaction parameter (dimensionless)
μ	nuclear magnetic moment (in units of μ_N)
μ_0	permeability of free space (henry m^{-1})
μ_B	Bohr magneton ($J T^{-1}$)
μ_N	nuclear magneton ($J T^{-1}$)
ω	frequency (s^{-1})
ω_D	Debye cutoff frequency (s^{-1})
ω_E	characteristic Einstein frequency (s^{-1})
$\hbar$	Planck's constant h divided by 2π (J s)

Spin Density Waves and Magnons

N Harrison, Los Alamos National Laboratory, Los Alamos, NM, USA

Introduction

A review of semiconductors would be incomplete without the inclusion of those classes of extremely narrow gap semiconductors and semimetals that result from microscopic interactions between itinerant (or nearly free) electrons in a correlated metal. This article is devoted to spin-density waves, which are a consequence of Coulomb interactions between electrons causing a system to become antiferromagnetic, which would otherwise be metallic. Perhaps, the most extreme example is that where the Coulomb interactions between electrons exceed the total electronic bandwidth, leading to an insulator that can be very well described by the Hubbard model. Spin-density waves are subtle by comparison, being much more dependent on details of the Fermi surface topology. It is, therefore, more convenient to consider spin-density waves as perturbations of electronic bands of quasiparticles in a metal. The gaps are